Flat Slab Subduction at the Middle American Subduction Zone in Central Mexico Determined from Receiver Function Analysis

YoungHee Kim and Robert W. Clayton

Seismological Laboratory, California Institute of Technology, Pasadena, California 91125

Email: {ykim, clay}@gps.caltech.edu

1 Abstract

The flat slab subduction of the Cocos plate beneath central Mexico is determined from the receiver functions (RFs) utilizing data from the Meso America Subduction Experiment (MASE). The RF image shows that the subducting oceanic crust is shallowly dipping to the north at 15° for 80 km from Acapulco and then horizontally underplates the continental crust for 200 km, from the trench to the southern extent of the Trans-Mexican Volcanic Belt (TMVB). The migrated image of the RFs shows that the slab is steeply dipping into the mantle at about 67° beneath the TMVB. Both the continental and oceanic Moho are clearly seen in both images. In particular, the RF image from Acapulco to a point 150 km to the north shows the erosion of the continental material by the slab. However, there is no apparent evidence of crustal compressional features supported by the geologic or geodetic data due to the underplating. Modeling of the RF conversion amplitudes and timings of the underplated feature indicates the need for a low-velocity zone between the plate and the continental crust. This may indicate melted upper crust or melted continental lithosphere.

2 Data

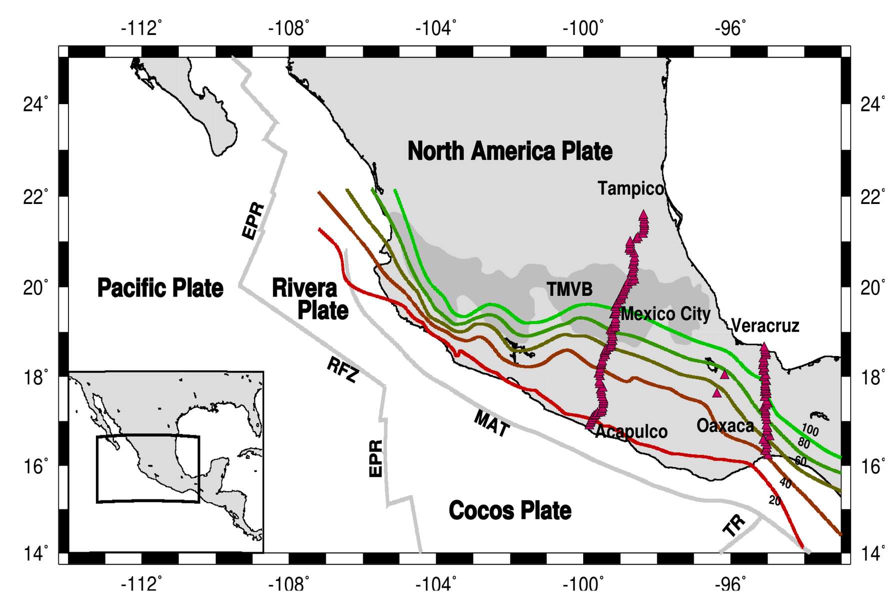

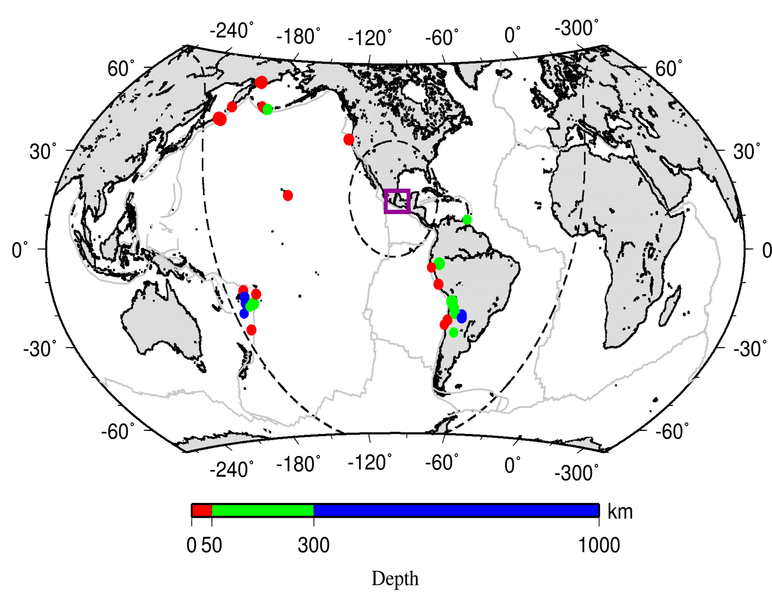

Map on the left shows the region of our study and stations in two MASE lines indicated as red triangles. Isodepth contours of the subducted Cocos plate beneath the North American plate (Pardo and Suarez, 1995) are shown in the map. Map on the right shows the distribution of teleseismic events used in the study. Dotted lines are distance of 30° and 90° away from the center of the study area. The events are colored in different colors according to depths.

3 Method: RF Stacking Algorithm and RF Migration

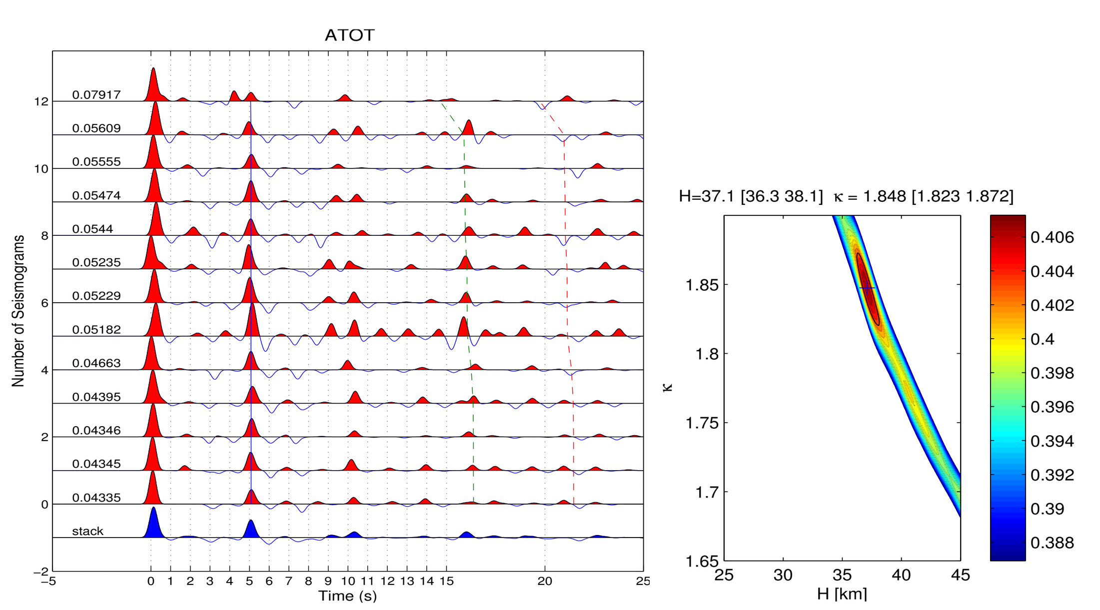

RF Stacking Algorithm

Crustal thickness (Moho, H) and Vp/Vs ratio (κ) for station ATOT (Atotonilco el Grande). On the left are the individual RF traces sorted according to the ray parameter. The predicted arrival times of the primary phase (Pms) and two multiples (PpPms and PsPms) are marked by the solid and dashed lines. On the right is the contour map of the weighted summation function (Zhu and Kanamori, 2000) for the crustal thickness (Moho, H) and Vp/Vs ratio (κ).

RF Migration

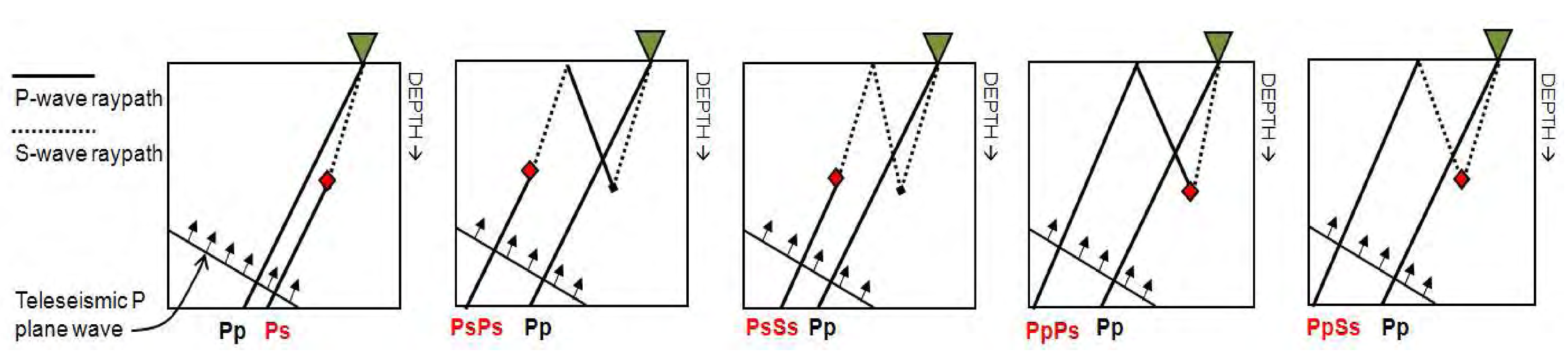

Plan view of geometry for several teleseimic wavefields. Incident plane wave is assumed to be P wave coming from a distant source; as hitting the scatterer, it converts to S wave to become Ps or other wavefields such as PsPs, PsSs, PpPs, or PpSs. Each wavefield is migrated using a Kirchhoff-style migration, which characterizes the ouput model as a grid of point scatters.

4 RF Results

(1) Anisotropic layers present in the crust

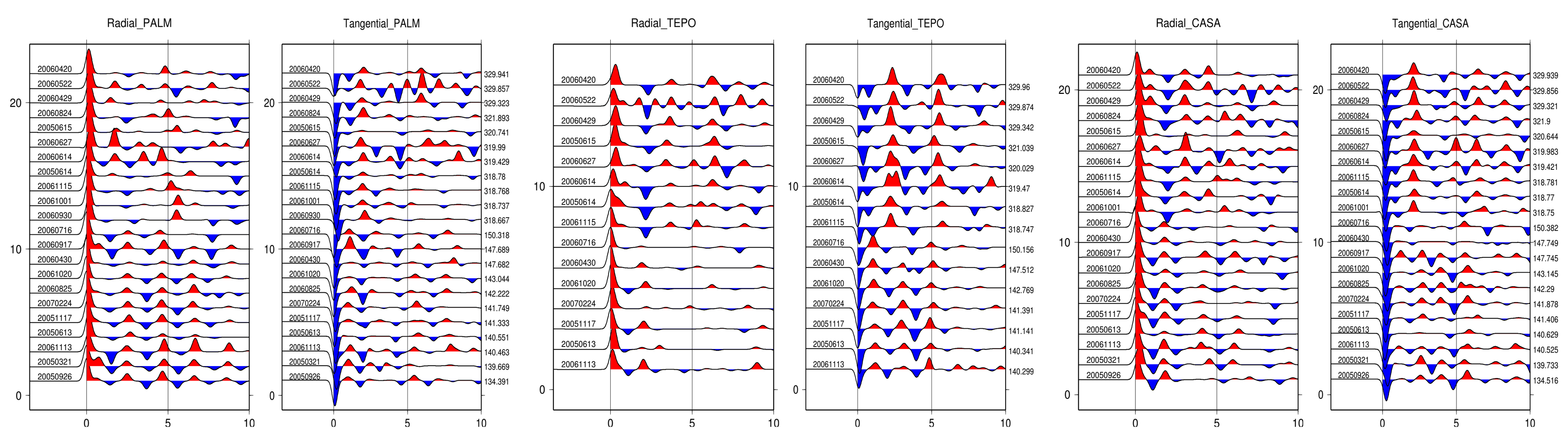

Radial and tangential RFs for station PALM, TEPO, and CASA. The radial and tangential RFs are computed by rotating NS component RF and EW component RF by 15° clockwise. For these particular stations, the RFs are plotted according to the back-azimuth. Note sudden changes in polarity (blue to red or red to blue) especially on the tangential RFs, indicating the anisotropic layers present at shallow depths.

(2) Stacked RF and migration results

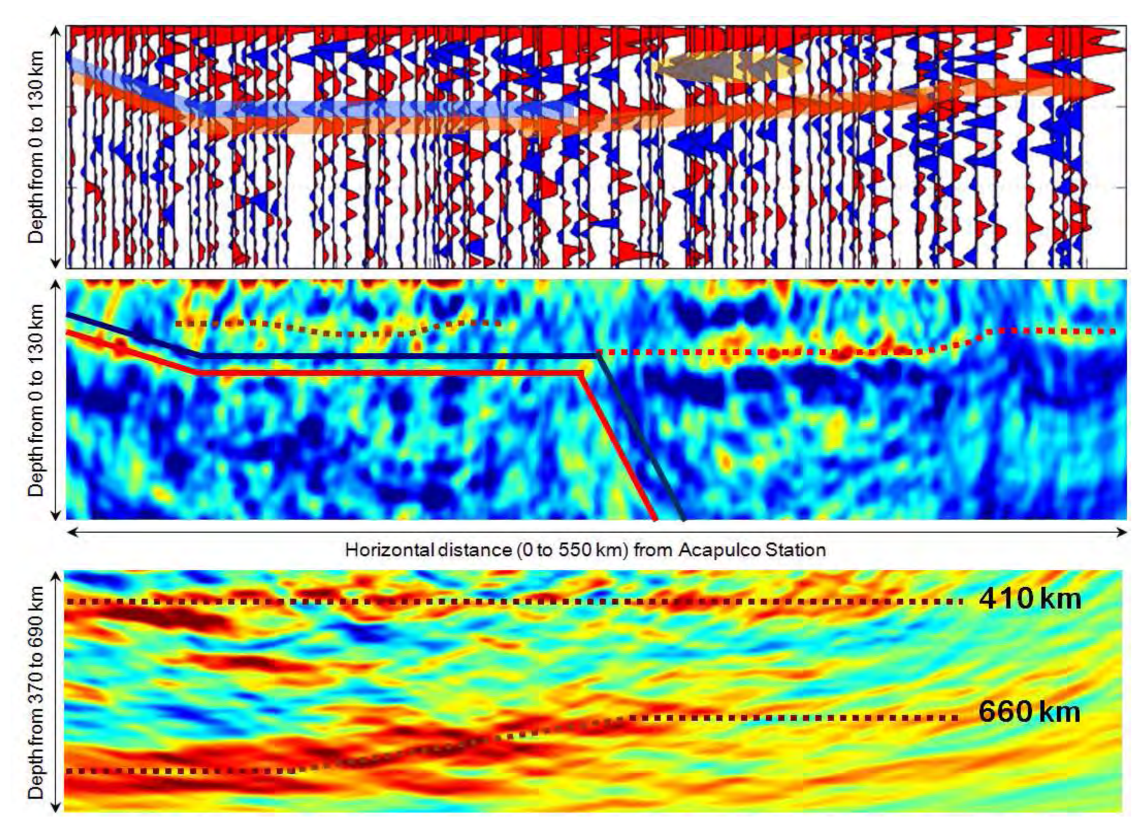

Stacked RFs using events from all directions (top), RF migration image from the surface to a depth of 130 km (middle), and migrated image of the upper mantle structure including 410 and 660 discontinuities (bottom). In the top panel, the blue interpretation segment shows the top of the subducting slab; the red segment the oceanic and continental Moho; and, the orange segment partial melting features from the TMVB. In the middle panel, the blue interpretation line shows the top of the subducting slab (a dip of 67° underneath the TMVB). The red line shows the bottom of the subducting slab; the dotted red line the continental Moho shallowing towards the north; and the dotted brown line mid-crustal interfaces. In the bottom panel, note the upward-moving trend of the 660 discontinuity underneath the TMVB suggesting an upwelling.

5 Modeling Result

P-wave velocity model for a steeply dipping slab

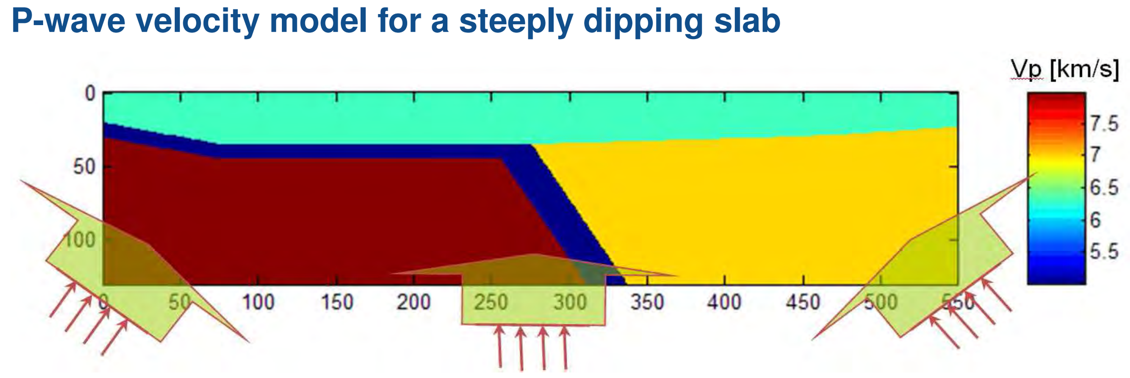

P-wave and S-wave velocity and density models are necessary to generate synthetic RF using a 2D finite-difference wave propagation program (Graves, 1996). We let plane waves with variable incident angles in the range of ray parameters from 0.04 to 0.08 enter from the bottom of the three models.

Migrated image using synthetic RFs compared with the one using real RFs

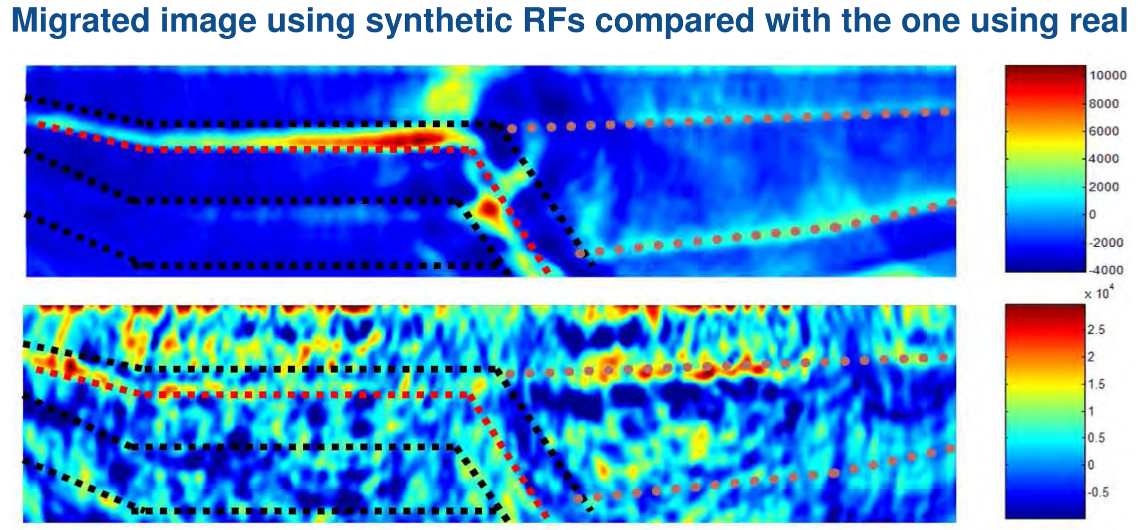

The migrated image using synthetic RFs includes primary and secondary conversions from the Moho and the slab. Especially, the oceanic Moho with the multiples, the continental Moho with the multiples, and the downgoing slab are well captured. To note, the migrated image using real RFs includes more complicated features like mid-crustal interfaces and basin on the TMVB, which we did not include for the synthetic test.

6 Preliminary Result on Velocity Models for the Flat Slab

RFs using earthquakes from SE dir (left) and from NW dir (right)

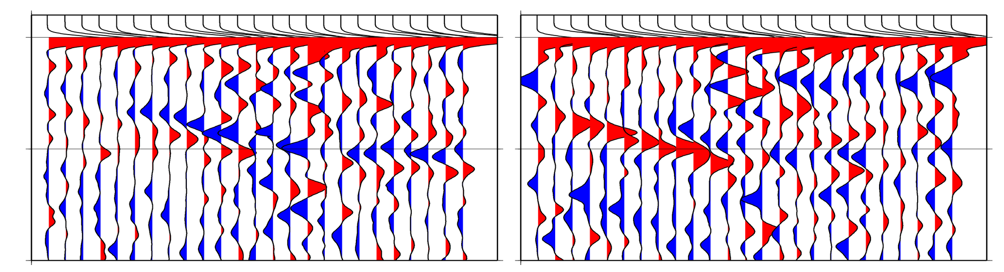

Synthetic RFs using sources from LHS (left) and from RHS (right)

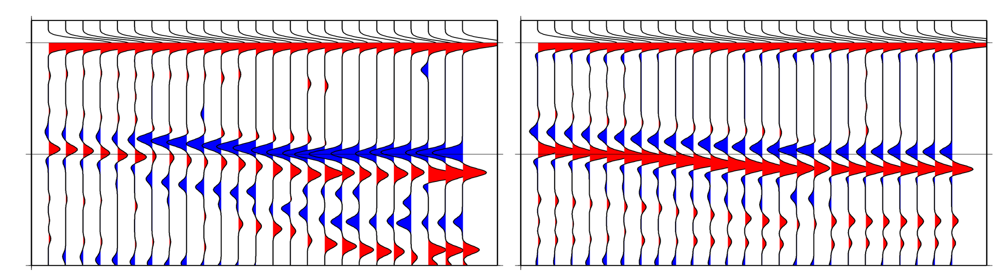

Two velocity models constructed to generate synthetic RFs

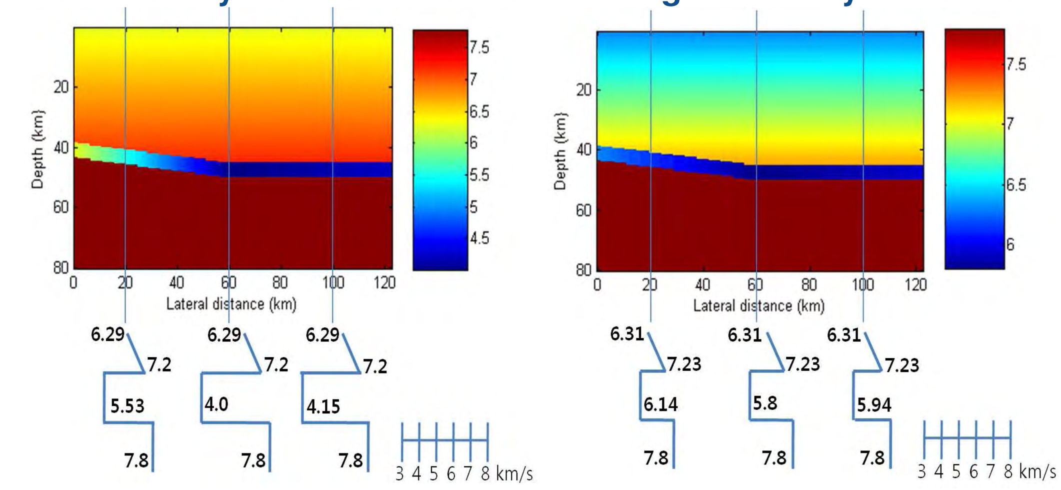

The subducted Cocos plate as imaged with RFs underplates the continental crust for a distance of approximately 300 km from the trench. Two different velocity models for the flat slab are constructed by considering the azimuthal dependence of the RF images (bottom panel). In the top panel, we show stacked RFs using events from the SE direction (left) and the NW direction (right). We observe that the image of the top of the slab appears to be strong from the RFs using events from the SE direction, and the image of the oceanic Moho appears to be strong from the RFs using events from the NW direction. In generating synthetic RFs (middle panel), we match impedane changes of the interface between the crust and the slab by measuring RF amplitudes and timing of the RF peak arrivals from the Moho and the slab. We ignore complicated structures within the crust (e.g., mid-crustal interfaces and basin structure near the surface). We include the vertical gradient in velocity within the crust and the horizontal gradient in velocity in the slab. A low velocity zone (lower than normal oceanic crustal velocities) might be necessary to reproduce impedance contrasts that we are not resolving at the moment.

7 Discussion / Conclusions / Future Work

1. We have obtained RF images of crustal structures associated with tectonic history of subducted Cocos plate beneath central Mexico for the first MASE line.
   - Flat slab subduction from the Pacific coast to the southern extent of TMVB
     - The subducting oceanic crust is shallow, dipping to the north at 15°, for 80 km from Acapulco.
     - There is no compressional feature on surface due to the underplating according to geologic or geodetic data.
     - The continental Moho is about 40 km deep beneath the TMVB and shallows towards the north.
   - Strong low velocity zone underneath the TMVB
     - There is apparent maximum attenuation at the top of the dipping slab
   - Steeply dipping (approximately 67°) slab underneath the TMVB
     - The slab geometry supports the idea of slab roll-back.

2. For the future work, we process seismograms recorded from the second MASE line (VEOX) to generate the RFs.

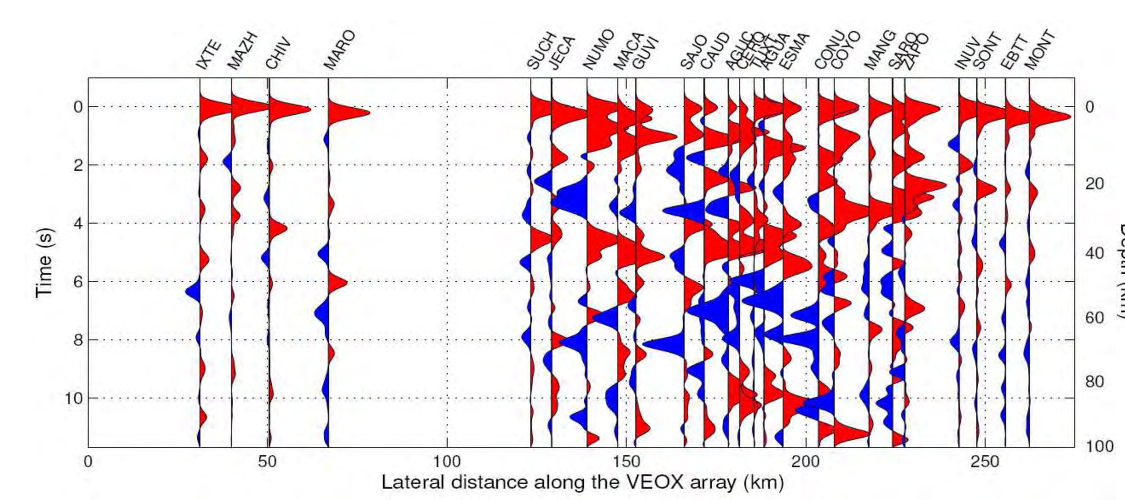

5 events (07/2007 to 08/2007) occurred on the SE direction from the VEOX array and 27 (out of 46) stations are used. The figure shows the stacked RFs plotted from the surface to a depth of 100 km. The slab geometry is not yet determined due to lack of data and limited number of fully operating stations, but the Moho is clear. Note that the Moho appears to be shallowing towards the north like we saw from the first MASE line.

8 References

- Graves, R.W., 1996. Simulating seismic wave propagation in 3D elastic media using staggered grid finite difference, Bull. Seism. Soc. Am., 86, 1,091-1,106.
- Pardo, M., and Suarez G., 1995. Shape of the subducted Rivera and Cocos plates in southern Mexico: Seismic and tectonic implications, J. Geophys. Res., 100, 12,357-12,373.
- Zhu, L. and Kanamori, H., 2000. Moho Depth Variation in Southern California from Teleseismic Receiver Functions, J. Geophys. Res., 105, 2, 969-2,980.